

# Supersymmetric electroweak corrections to bottom squark decay into a lighter top squark and charged Higgs boson

Li Gang Jin and Chong Sheng Li

*Department of Physics, Peking University, Beijing 100871, People's Republic of China*

(Received 22 June 2001; revised manuscript received 28 September 2001; published 10 January 2002)

The Yukawa corrections of order  $\mathcal{O}(\alpha_{ew}m_{t(b)}^2/m_W^2)$ ,  $\mathcal{O}(\alpha_{ew}m_{t(b)}^3/m_W^3)$ , and  $\mathcal{O}(\alpha_{ew}m_{t(b)}^4/m_W^4)$  to the width of bottom squark decay into a lighter top squark plus a charged Higgs boson are calculated in the minimal supersymmetric standard model. These corrections depend on the masses of the charged Higgs boson and lighter top squark and the parameters  $\tan\beta$  and  $\mu$ . For favorable parameter values, the corrections decrease or increase the decay widths significantly. In particular, for high values of  $\tan\beta$  ( $=30$ ) the corrections exceed 10% for both  $\tilde{b}_1$  and  $\tilde{b}_2$  decay. But for low values of  $\tan\beta$  ( $=4,10$ ) the corrections are small and the magnitudes are less than 10%. The numerical calculations also show that using the running bottom quark mass, which includes the QCD effects and resums all high order ( $\tan\beta$ )-enhanced effects can vastly improve the convergence of the perturbation expansion.

DOI: 10.1103/PhysRevD.65.035007

PACS number(s): 14.80.Ly, 12.38.Bx, 14.80.Cp

## I. INTRODUCTION

The minimal supersymmetric standard model (MSSM) [1,2] is an attractive extension of the standard model (SM). In this model every quark has two spin zero partners called squarks,  $\tilde{q}_L$  and  $\tilde{q}_R$ , one for each chirality eigenstate. These current eigenstates mix to form the mass eigenstates  $\tilde{q}_1$  and  $\tilde{q}_2$ . The third generation squarks are of special interest. This is mainly for the following reasons: Large Yukawa couplings lead to strong mixing which induces large mass differences between the lighter mass eigenstate and the heavier one. This implies in general a very complex decay pattern of the heavier states. The dominant decay modes of the heavier squarks are the decays into quarks plus charginos or neutralinos, decays into lighter squarks plus vector bosons, and decays into lighter squarks plus Higgs bosons. All these squark decays have been extensively discussed at the tree level [3–5]. The next generation of colliders, for example, the CERN Large Hadron Collider (LHC), will be able to produce such kinds of particles with masses up to 2.5 TeV [6], and a  $e^+e^-$  linear collider [7] will be able to make precise measurements of their properties. Thus a more accurate calculation of the decay mechanisms beyond the tree level is necessary in order to provide a solid basis for experimental analysis to observe these decays at the next generation of colliders. Up to now, one-loop QCD and supersymmetric (SUSY) QCD corrections to the squark decays have been calculated [4,8], and the Yukawa corrections to the squark decays into quarks plus charginos or neutralinos were also given in Ref. [9]. Very recently, a complete one-loop computation of the electroweak radiative corrections to the above processes has been presented by Guasch, Hollik, and Solà [10]. But the electroweak radiative corrections to the heavier squark decays into lighter squarks plus vector bosons and decays into lighter squarks plus Higgs bosons have not been calculated yet, including the Yukawa corrections to these processes. In this paper, we present calculations of the Yukawa corrections of order  $\mathcal{O}(\alpha_{ew}m_{t(b)}^2/m_W^2)$ ,  $\mathcal{O}(\alpha_{ew}m_{t(b)}^3/m_W^3)$ , and  $\mathcal{O}(\alpha_{ew}m_{t(b)}^4/m_W^4)$  to the width of bot-

tom squark decay into a lighter top squark plus a charged Higgs boson, i.e., the decay  $\tilde{b}_i \rightarrow \tilde{t}_1 + H^-$ , where  $\tilde{t}_1$  is the lighter top squark. These corrections are mainly induced by Yukawa couplings from Higgs boson–quark–quark couplings, Higgs boson–squark–squark couplings, Higgs boson–Higgs boson–squark–squark couplings, chargino–(neutralino–) quark–squark couplings, and squark–squark–squark–squark couplings.

Our results can be generalized straightforwardly to the decay  $\tilde{t}_2 \rightarrow \tilde{t}_1 + (h^0, A^0)$ . As for the heavier squark decays into lighter squarks plus vector bosons, the electroweak radiative corrections are simple because of the smaller number of renormalization parameters involved.

## II. NOTATION AND TREE-LEVEL RESULT

In order to make this paper self-contained, we first summarize our notation and present the relevant interaction Lagrangians of the MSSM and the tree-level decay rates for  $\tilde{b}_i \rightarrow \tilde{t}_1 + H^-$ .

The current eigenstates  $\tilde{q}_L$  and  $\tilde{q}_R$  are related to the mass eigenstates  $\tilde{q}_1$  and  $\tilde{q}_2$  by

$$\begin{pmatrix} \tilde{q}_1 \\ \tilde{q}_2 \end{pmatrix} = R^{\tilde{q}} \begin{pmatrix} \tilde{q}_L \\ \tilde{q}_R \end{pmatrix}, \quad R^{\tilde{q}} = \begin{pmatrix} \cos\theta_{\tilde{q}} & \sin\theta_{\tilde{q}} \\ -\sin\theta_{\tilde{q}} & \cos\theta_{\tilde{q}} \end{pmatrix} \quad (1)$$

with  $0 \leq \theta_{\tilde{q}} < \pi$  by convention. Correspondingly, the mass eigenvalues  $m_{\tilde{q}_1}^2$  and  $m_{\tilde{q}_2}^2$  (with  $m_{\tilde{q}_1} \leq m_{\tilde{q}_2}$ ) are given by

$$\begin{pmatrix} m_{\tilde{q}_1}^2 & 0 \\ 0 & m_{\tilde{q}_2}^2 \end{pmatrix} = R^{\tilde{q}} M_{\tilde{q}}^2 (R^{\tilde{q}})^\dagger, \quad M_{\tilde{q}}^2 = \begin{pmatrix} m_{\tilde{q}_L}^2 & a_q m_q \\ a_q m_q & m_{\tilde{q}_R}^2 \end{pmatrix} \quad (2)$$

with

$$m_{\tilde{q}_L}^2 = M_{\tilde{Q}}^2 + m_q^2 + m_Z^2 \cos 2\beta (I_{3L}^q - e_q \sin^2 \theta_W), \quad (3)$$

$$m_{q_R}^2 = M_{\{\tilde{U}, \tilde{D}\}}^2 + m_q^2 + m_Z^2 \cos 2\beta e_q \sin^2 \theta_W, \quad (4)$$

$$a_q = A_q - \mu \{\cot \beta, \tan \beta\} \quad (5)$$

for {up,down} type squarks. Here  $M_q^2$  is the squark mass matrix.  $M_{\tilde{Q}, \tilde{U}, \tilde{D}}$  and  $A_{t,b}$  are soft supersymmetric breaking parameters and  $\mu$  is the Higgs boson mixing parameter in the superpotential.  $I_{3L}^q$  and  $e_q$  are the third component of the weak isospin and the electric charge of the quark  $q$ , respectively.

Defining  $H_k = (h^0, H^0, A^0, G^0, H^\pm, G^\pm)$  ( $k=1, \dots, 6$ ), one can write the relevant Lagrangian density in the  $(\tilde{q}_1, \tilde{q}_2)$  basis in the following form ( $i, j=1, 2$ ;  $\alpha$  and  $\beta$  are flavor indices):

$$\begin{aligned} \mathcal{L}_{\text{relevant}} = & H_k \bar{q}^\beta (a_k^\alpha P_L + b_k^\alpha P_R) q^\alpha + (G_k^\alpha)_{ij} H_k \tilde{q}_j^{\beta*} \tilde{q}_i^\alpha \\ & + g \bar{q} (a_{ik}^\alpha P_R + b_{ik}^\alpha) \tilde{\chi}_k^0 \tilde{q}_i + g \bar{t} (l_{ik}^b P_R + k_{ik}^b P_L) \tilde{\chi}_k^+ \tilde{b}_i \end{aligned}$$

$$\begin{aligned} & + g \bar{b} (l_{ik}^t P_R + k_{ik}^t P_L) \tilde{\chi}_k^{+c} \tilde{t}_i \\ & + (G_{5k}^\alpha)_{ij} H^+ H_k \tilde{q}_j^{\beta*} \tilde{q}_i^\alpha + \text{H.c.}, \end{aligned} \quad (6)$$

with

$$\begin{aligned} (G_k^\alpha)_{ij} = & [R^\alpha \hat{G}_k^\alpha (R^\beta)^T]_{ij}, \quad (G_{5k}^\alpha)_{ij} = [R^\alpha \hat{G}_{5k}^\alpha (R^\beta)^T]_{ij} \\ & (k=1, \dots, 6), \end{aligned} \quad (7)$$

where  $\hat{G}_k^\alpha$  and  $\hat{G}_{5k}^\alpha$  are the couplings in the  $(\tilde{q}_L, \tilde{q}_R)$  basis, and their explicit forms are shown in Appendix A. The notations  $a_k^\alpha, b_k^\alpha$  ( $k=1, \dots, 6$ ) and  $a_{ik}^\alpha, b_{ik}^\alpha$  ( $k=1, \dots, 4$ ), and  $l_{ik}^\alpha, k_{ik}^\alpha$  ( $k=1, 2$ ) used in Eq. (6) are also defined in Appendix A.

The tree-level amplitude of  $\tilde{b}_i \rightarrow \tilde{t}_1 H^-$ , as shown in Fig. 1(a), is given by

$$M_i^{(0)} = \frac{ig}{\sqrt{2}m_W} \left[ R^b \begin{pmatrix} m_b^2 \tan \beta + m_t^2 \cot \beta - m_W^2 \sin 2\beta & m_t (A_t \cot \beta + \mu) \\ m_b (A_b \tan \beta + \mu) & 2m_t m_b / \sin 2\beta \end{pmatrix} (R^t)^T \right]_{i1}, \quad (8)$$

and the decay width is

$$\Gamma_i^{(0)} = \frac{|M_i^{(0)}|^2 \lambda^{1/2}(m_{\tilde{b}_i}^2, m_{\tilde{t}_1}^2, m_{H^-}^2)}{16\pi m_{\tilde{b}_i}^3} \quad (9)$$

with  $\lambda(x, y, z) = (x - y - z)^2 - 4yz$ .

### III. YUKAWA CORRECTIONS

The Feynman diagrams contributing to the Yukawa corrections to  $\tilde{b}_i \rightarrow \tilde{t}_1 H^-$  are shown in Figs. 1(b)–1(f) and Fig. 2. We carried out the calculation in the 't Hooft–Feynman gauge and used dimensional reduction, which preserves supersymmetry, for regularization of the ultraviolet divergences in the virtual loop corrections using the on-mass-shell renormalization scheme [11], in which the fine-structure constant  $\alpha_{ew}$  and physical masses are chosen to be the renormalized parameters, and the finite parts of the counterterms are fixed by the renormalization conditions. The coupling constant  $g$  is related to the input parameters  $e$ ,  $m_W$ , and  $m_Z$  via  $g^2 = e^2/s_w^2$  and  $s_w^2 = 1 - m_W^2/m_Z^2$ . As for the renormalization of the parameters in the Higgs boson sector and the squark sector, it will be described in detail below.

The relevant renormalization constants are defined as

$$m_{W0}^2 = m_W^2 + \delta m_W^2, \quad m_{Z0}^2 = m_Z^2 + \delta m_Z^2, \quad (10)$$

$$m_{q0} = m_q + \delta m_q, \quad m_{\tilde{q}_i0}^2 = m_{\tilde{q}_i}^2 + \delta m_{\tilde{q}_i}^2,$$

$$A_{q0} = A_q + \delta A_q, \quad \mu_0 = \mu + \delta \mu,$$

$$\theta_{\tilde{q}0} = \theta_q + \delta \theta_{\tilde{q}}, \quad \tan \beta_0 = (1 + \delta Z_\beta) \tan \beta,$$

$$\tilde{q}_{i0} = (1 + \delta Z_{\tilde{q}_i}^2)^{1/2} + \delta Z_{ij}^{\tilde{q}} \tilde{q}_j,$$

$$H_0^- = (1 + \delta Z_{H^-})^{1/2} H^- + \delta Z_{HG} G^-,$$

$$G_0^- = (1 + \delta Z_{G^-})^{1/2} G^- + \delta Z_{GH} H^-$$

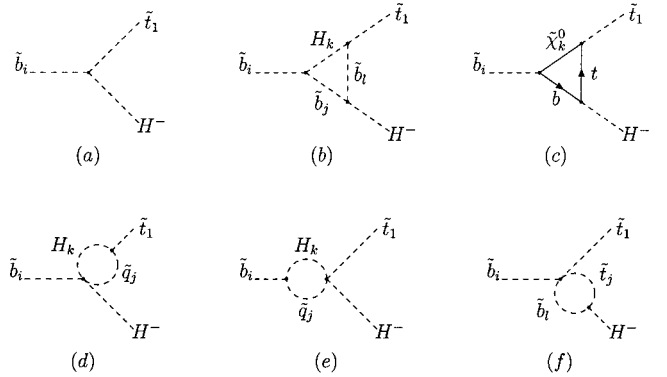


FIG. 1. Feynman diagrams contributing to supersymmetric electroweak corrections to  $\tilde{b}_i \rightarrow \tilde{t}_1 H^-$ : (a) tree-level diagram; (b)–(f) one-loop vertex corrections. In (b) the subscript  $k$  of  $H_k$  can take values from 1 to 4. In (d)  $q=t$  for  $k=1, \dots, 4$  and  $q=b$  for  $k=5, 6$ . In (e)  $q=b$  for  $k=1, \dots, 4$  and  $q=t$  for  $k=5, 6$ .

with  $q=t,b$ . Here we introduce the mixing of  $H^-$  and  $G^-$  [12], instead of the mixing of  $H^-$  and  $W^-$  [13],

$$\begin{aligned} W_{\mu 0}^- &= (1 + \delta Z_{W^-})^{1/2} W_{\mu}^- + i Z_{WH} \partial_{\mu} H^-, \\ H_0^- &= (1 + \delta Z_{H^-})^{1/2} H^-, \end{aligned} \quad (11)$$

for the following reason: the former can successfully cancel the divergences for the case we are considering, but the latter is right only for the renormalization of the parameters  $\beta$  and  $\alpha$ , and in the case that the particles interacting with the charged Higgs boson are the on-shell fermions (where a  $\not{p}$  arising from  $\partial_{\mu} H^-$  and the vertex  $W^-$ -fermion-fermion is

inserted between two on-shell fermions, and turned into the fermion masses by Dirac equations, which is therefore similar to the structure of the Yukawa coupling  $H^-$ -fermion-fermion).

Taking into account the Yukawa corrections, the renormalized amplitude for  $\tilde{b}_i \rightarrow \tilde{t}_1 H^-$  is given by

$$M_i^{\text{ren}} = M_i^{(0)} + \delta M_i^{(v)} + \delta M_i^{(c)}, \quad (12)$$

where  $\delta M_i^{(v)}$  and  $\delta M_i^{(c)}$  are the vertex corrections and the counterterm, respectively.

The calculations of the vertex corrections from Figs. 1(b)–1(f) result in

$$\begin{aligned} \delta M_i^{(v)} &= \frac{i}{16\pi^2} \sum_{k=1}^6 \sum_j (G_{5k}^{\tilde{b}})_{ij} (G_k^{\tilde{b}})_{j1} B_0(p_{\tilde{t}_1}, m_{H_k}, m_{\tilde{q}_j}) + \frac{i}{16\pi^2} \sum_{k=1}^6 \sum_j (G_k^{\tilde{b}})_{ij} (G_{5k}^{\tilde{b}})_{j1} B_0(p_{\tilde{b}_i}, m_{H_k}, m_{\tilde{q}_j}) \\ &\quad - \frac{i}{16\pi^2} \sum_{k=1}^4 \sum_{j,l} (G_k^{\tilde{b}})_{ij} (G_5^{\tilde{b}})_{jl} (G_k^{\tilde{t}})_{l1} C_0(-p_{\tilde{b}_i}, p_{H^-}, m_{H_k}, m_{\tilde{b}_j}, m_{\tilde{t}_l}) + \frac{ig^2}{8\pi^2} \sum_{k=1}^4 \{ [m_t m_b a_5^b + (m_{\tilde{b}_i}^2 - p_{\tilde{b}_i} \cdot p_{H^-}) b_5^b] \\ &\quad \times m_{\tilde{\chi}_k^0} b_{ik}^{\tilde{b}} a_{1k}^{\tilde{t}*} C_0 + b_{ik}^{\tilde{b}} [m_b a_5^b b_{1k}^{\tilde{t}*} (p_{\tilde{b}_i} - p_{H^-}) + m^t b_5^b b_{1k}^{\tilde{t}*} p_{\tilde{b}_i} - m_{\tilde{\chi}_k^0} b_5^b a_{1k}^{\tilde{t}*} (2p_{\tilde{b}_i} - p_{H^-})]_{\mu} (-p_{\tilde{b}_i}^{\mu} C_{11} + p_{H^-}^{\mu} C_{12}) \\ &\quad - (m_b a_5^b b_{1k}^{\tilde{t}*} + m_t b_5^b b_{1k}^{\tilde{t}*} - m_{\tilde{\chi}_k^0} b_5^b a_{1k}^{\tilde{t}*}) b_{ik}^{\tilde{b}} (m_{\tilde{b}_i}^2 C_{21} + m_{H^-}^2 C_{22} - 2p_{\tilde{b}_i} \cdot p_{H^-} C_{23} + g_{\mu}^{\mu} C_{24}) + (a \leftrightarrow b) \} \\ &\quad \times (-p_{\tilde{b}_i}, p_{H^-}, m_{\tilde{\chi}_k^0}, m_b, m_t) - \frac{3i}{16\pi^2} \sum_{j,l} (h_b^2 R_{12}^{\tilde{b}} R_{i2}^{\tilde{b}} R_{j1}^{\tilde{t}} R_{l1}^{\tilde{t}} + h_t^2 R_{i1}^{\tilde{b}} R_{l1}^{\tilde{b}} R_{12}^{\tilde{t}} R_{j2}^{\tilde{t}}) (G_5^{\tilde{b}})_{ij} B_0(p_{H^-}, m_{\tilde{b}_i}, m_{\tilde{t}_j}), \end{aligned} \quad (13)$$

where  $B_0$  and  $C_{i(j)}$  are two- and three-point Feynman integrals [14], respectively, and  $h_{i(b)}$  is the Yukawa coupling defined by

$$h_t = \frac{gm_t}{\sqrt{2}m_W \sin \beta}, \quad h_b = \frac{gm_b}{\sqrt{2}m_W \cos \beta}. \quad (14)$$

In the first term of  $\delta M_i^{(v)}$ ,  $q=t$  for  $k=1, \dots, 4$  and  $q=b$  for  $k=5, 6$ , while in the second term,  $q=b$  for  $k=1, \dots, 4$  and  $q=t$  for  $k=5, 6$ .

The counterterm can be expressed as

$$\begin{aligned} \delta M_i^{(c)} &= i(\delta\theta_{\tilde{b}} + \delta Z_{21}^{\tilde{b}}) (G_5^{\tilde{b}})_{3-i,1} + i(\delta\theta_{\tilde{t}} + \delta Z_{21}^{\tilde{t}}) (G_5^{\tilde{b}})_{i2} \\ &\quad + i[R^{\tilde{b}}(\delta\hat{G}_5^{\tilde{b}})(R^{\tilde{t}})^T]_{i1} + \frac{i}{2}(\delta Z_i^{\tilde{b}} + \delta Z_1^{\tilde{t}} + \delta Z_{H^-}) \\ &\quad \times (G_5^{\tilde{b}})_{i1} + i\delta Z_{GH} (G_6^{\tilde{b}})_{i1} \end{aligned} \quad (15)$$

with

$$\begin{aligned} (\delta\hat{G}_5^{\tilde{b}})_{11} &= \frac{g}{\sqrt{2}m_W} \left[ \left( \frac{\delta g}{g} - \frac{1}{2} \frac{\delta m_W^2}{m_W^2} \right) (m_b^2 \tan \beta + m_t^2 \cot \beta) \right. \\ &\quad \left. + 2m_b \tan \beta \delta m_b + 2m_t \cot \beta \delta m_t + m_b^2 \delta \tan \beta \right. \\ &\quad \left. + m_t^2 \cot \beta \right], \end{aligned} \quad (16)$$

$$\begin{aligned} (\delta\hat{G}_5^{\tilde{b}})_{12} &= \frac{g}{\sqrt{2}m_W} \left[ \left( \frac{\delta g}{g} - \frac{1}{2} \frac{\delta m_W^2}{m_W^2} + \frac{\delta m_t}{m_t} \right) m_t (A_t \cot \beta + \mu) \right. \\ &\quad \left. + m_t (\delta A_t \cot \beta + A_t \delta \cot \beta + \delta \mu) \right], \end{aligned} \quad (17)$$

$$\begin{aligned} (\delta\hat{G}_5^{\tilde{b}})_{21} &= \frac{g}{\sqrt{2}m_W} \left[ \left( \frac{\delta g}{g} - \frac{1}{2} \frac{\delta m_W^2}{m_W^2} + \frac{\delta m_b}{m_b} \right) m_b (A_b \tan \beta + \mu) \right. \\ &\quad \left. + m_b (\delta A_b \tan \beta + A_b \delta \tan \beta + \delta \mu) \right], \end{aligned} \quad (18)$$

$$\begin{aligned} (\delta\hat{G}_5^{\tilde{b}})_{22} &= \frac{2gm_b m_t}{\sqrt{2}m_W \sin 2\beta} \left( \frac{\delta g}{g} - \frac{1}{2} \frac{\delta m_W^2}{m_W^2} + \frac{\delta m_b}{m_b} + \frac{\delta m_t}{m_t} \right. \\ &\quad \left. - \cos 2\beta \delta Z_{\beta} \right). \end{aligned} \quad (19)$$

Here we consider only the corrections to the Yukawa couplings. The explicit expressions for some renormalization constants calculated from the self-energy diagrams in Fig. 2 are given in Appendix B, and other renormalization constants are fixed as follows.

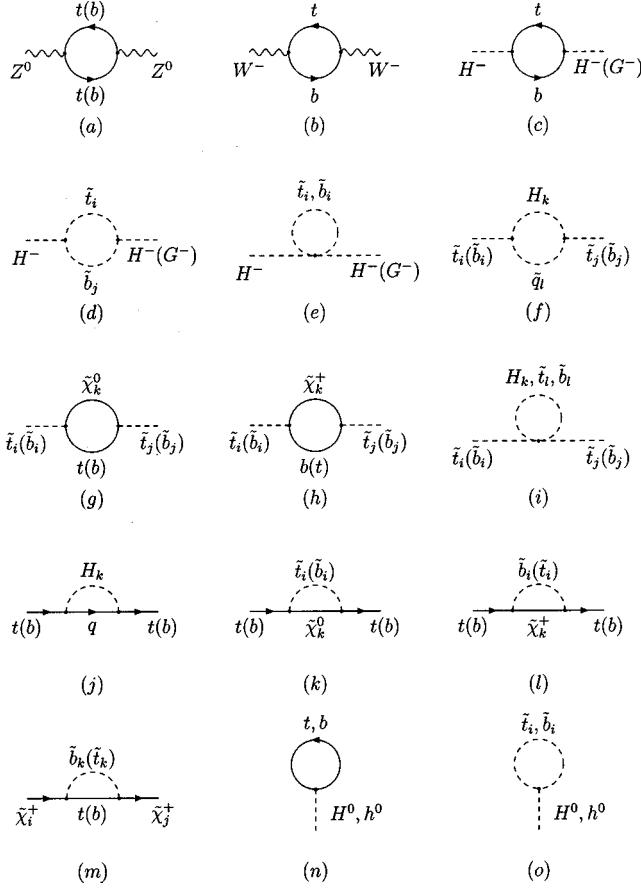


FIG. 2. Feynman diagrams contributing to renormalization constants. In (i)  $q=t(b)$  for  $k=1, \dots, 4$  and  $q=b(t)$  for  $k=5,6$ .

For  $\delta Z_{GH}$ , using the approach discussed in the two-Higgs-doublet model in [12], we derive below its expression in the MSSM, where the version of the Higgs potential is different from that of Ref. [12]. First, the one-loop renormalized two-point function is given by

$$i\Gamma_{GH}(p^2) = i(p^2 - m_{H^-}^2)\delta Z_{HG} + ip^2\delta Z_{GH} - iT_{GH} + i\Sigma_{GH}(p^2), \quad (20)$$

where  $T_{GH}$  is the tadpole function, which is given by

$$T_{GH} = \frac{g}{2m_W} [T_{H_2} \sin(\alpha - \beta) + T_{H_1} \cos(\alpha - \beta)]. \quad (21)$$

Next, from the on-shell renormalization condition, we obtain

$$\delta Z_{GH} = \frac{1}{m_{H^-}^2} [T_{GH} - \Sigma_{GH}(m_{H^-}^2)]. \quad (22)$$

The explicit expressions for  $\Sigma_{GH}$  and the tadpole counterterms  $T_{H_k}$  ( $k=1,2$ ) are given in Appendix B.

For renormalization of the parameter  $\beta$ , following the analysis of Ref. [13], we fixed the renormalization constant by the requirement that the on-mass-shell  $H^+ \bar{\nu} \nu$  coupling retain the same form as in Eq. (3) of Ref. [13] to all orders of

perturbation theory. However, by introducing the mixing of  $H^-$  and  $G^-$  instead of  $H^-$  and  $W^-$ , the expression for  $\delta Z_\beta$  is changed to

$$\delta Z_\beta = \frac{1}{2} \frac{\delta m_W^2}{m_W^2} - \frac{1}{2} \frac{\delta m_Z^2}{m_Z^2} + \frac{1}{2} \frac{\delta m_Z^2 - \delta m_W^2}{m_Z^2 - m_W^2} - \frac{1}{2} \delta Z_{H^+} + \cot \beta \delta Z_{GH}. \quad (23)$$

For the counterterm of the squark mixing angle  $\theta_{\bar{q}}$ , using the same renormalization scheme as Ref. [9], one has

$$\delta \theta_{\bar{q}} = \frac{\text{Re}[\Sigma_{12}^{\bar{q}}(m_{\bar{q}_1}^2) + \Sigma_{12}^{\bar{q}}(m_{\bar{q}_2}^2)]}{2(m_{\bar{q}_1}^2 - m_{\bar{q}_2}^2)}. \quad (24)$$

For the renormalization of soft SUSY breaking parameter  $A_q$ , we fixed its counterterm by keeping the tree-level relation of  $A_q$ ,  $m_{\bar{q}_i}$ , and  $\theta_{\bar{q}}$  [15], and obtained the following expression:

$$\delta A_q = \frac{m_{\bar{q}_1}^2 - m_{\bar{q}_2}^2}{2m_q} \left( 2 \cos 2\theta_{\bar{q}} \delta \theta_{\bar{q}} - \sin 2\theta_{\bar{q}} \frac{\delta m_q}{m_q} \right) + \frac{\sin 2\theta_{\bar{q}}}{2m_q} (\delta m_{\bar{q}_1}^2 - \delta m_{\bar{q}_2}^2) + \{\cot \beta, \tan \beta\} \delta \mu + \delta \{\cot \beta, \tan \beta\} \mu. \quad (25)$$

As for the parameter  $\mu$ , there are several schemes [10,16,17] to fix its counterterm, and here we use the on-shell renormalization scheme of Ref. [17], which gives

$$\delta \mu = \sum_{k=1}^2 [m_{\bar{\chi}_k^+} (\delta U_{k2} V_{k2} + U_{k2} \delta V_{k2}) + \delta m_{\bar{\chi}_k^+} U_{k2} V_{k2}], \quad (26)$$

where  $(U, V)$  are the two  $2 \times 2$  matrices diagonalizing the chargino mass matrix, and their counterterms  $(\delta U, \delta V)$  are given by

$$\delta U = \frac{1}{4} (\delta Z_R - \delta Z_R^T) U, \quad (27)$$

$$\delta V = \frac{1}{4} (\delta Z_L - \delta Z_L^T) V. \quad (28)$$

The mass shifts  $\delta m_{\bar{\chi}_k^+}$  and the off-diagonal wave function renormalization constants  $\delta Z_{R(L)}$  can be written as

$$\delta m_{\bar{\chi}_k^+} = \frac{1}{2} \text{Re} \{ m_{\bar{\chi}_k^+} [\Pi_{kk}^L(m_{\bar{\chi}_k^+}^2) + \Pi_{kk}^R(m_{\bar{\chi}_k^+}^2)] + \Pi_{kk}^{S,L}(m_{\bar{\chi}_k^+}^2) + \Pi_{kk}^{S,R}(m_{\bar{\chi}_k^+}^2) \} \quad (29)$$

$$(\delta Z_R)_{ij} = \frac{2}{m_{\bar{\chi}_i^+}^2 - m_{\bar{\chi}_j^+}^2} \text{Re} [\Pi_{ij}^R(m_{\bar{\chi}_j^+}^2) m_{\bar{\chi}_j^+}^2 + \Pi_{ij}^L(m_{\bar{\chi}_j^+}^2) m_{\bar{\chi}_i^+} m_{\bar{\chi}_j^+} + \Pi_{ij}^{S,R}(m_{\bar{\chi}_j^+}^2) m_{\bar{\chi}_i^+} + \Pi_{ij}^{S,L}(m_{\bar{\chi}_j^+}^2) m_{\bar{\chi}_j^+}], \quad (30)$$

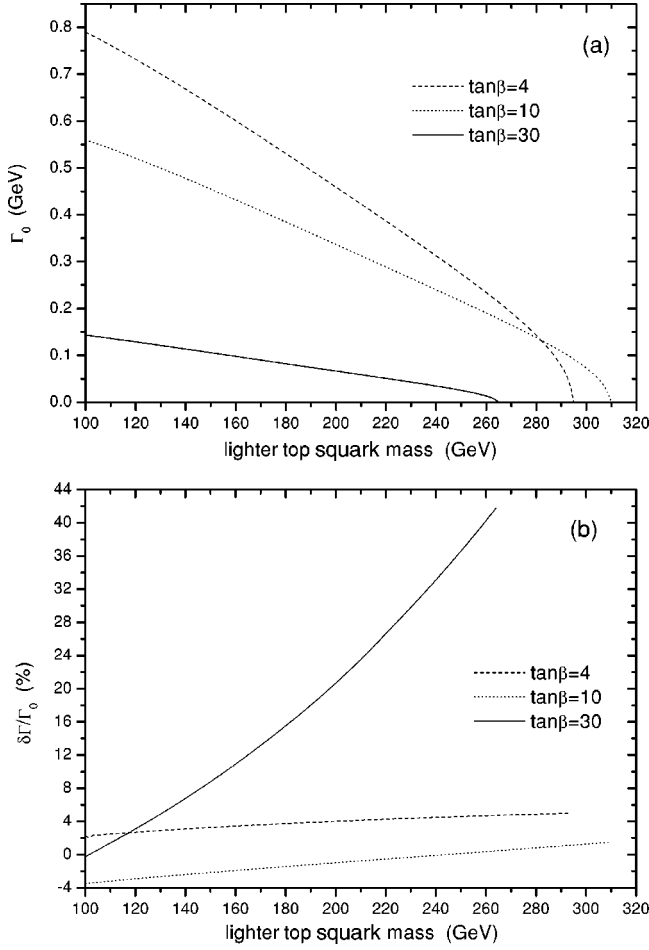


FIG. 3. The tree-level decay width (a) of  $\tilde{b}_1 \rightarrow \tilde{t}_1 H^-$  and its Yukawa corrections (b) as functions of  $m_{\tilde{t}_1}$  for  $\tan\beta = 4, 10$ , and  $30$ , assuming  $m_{A^0} = 150$  GeV,  $\mu = M_2 = 400$  GeV,  $A_t = A_b = 1$  TeV, and  $M_{\tilde{Q}} = M_{\tilde{U}} = M_{\tilde{D}}$ .

$$(\delta Z_L)_{ij} = (\delta Z_R)_{ij} \quad (L \leftrightarrow R). \quad (31)$$

The explicit expressions for the chargino self-energy matrices  $\Pi^{L(R)}$  and  $\Pi^{S,L(R)}$  are given in Appendix B.

Finally, the renormalized decay width is then given by

$$\Gamma_i = \Gamma_i^{(0)} + \delta\Gamma_i^{(v)} + \delta\Gamma_i^{(c)} \quad (32)$$

with

$$\delta\Gamma_i^{(a)} = \frac{\lambda^{1/2}(m_{\tilde{b}_i}^2, m_{\tilde{t}_1}^2, m_{H^-}^2)}{8\pi m_{\tilde{b}_i}^3} \text{Re}\{M_i^{(0)*} \delta M_i^{(a)}\} \quad (a = v, c). \quad (33)$$

#### IV. NUMERICAL RESULTS AND CONCLUSION

In the following we present some numerical results for the Yukawa corrections to bottom squark decay into a lighter top squark plus a charged Higgs boson. In our numerical calculations the SM parameters were taken to be  $\alpha_{ew}(m_Z) = 1/128.8$ ,  $m_W = 80.375$  GeV,  $m_Z = 91.1867$  GeV [18], and  $m_t = 175.6$  GeV. In order to improve the convergence of the

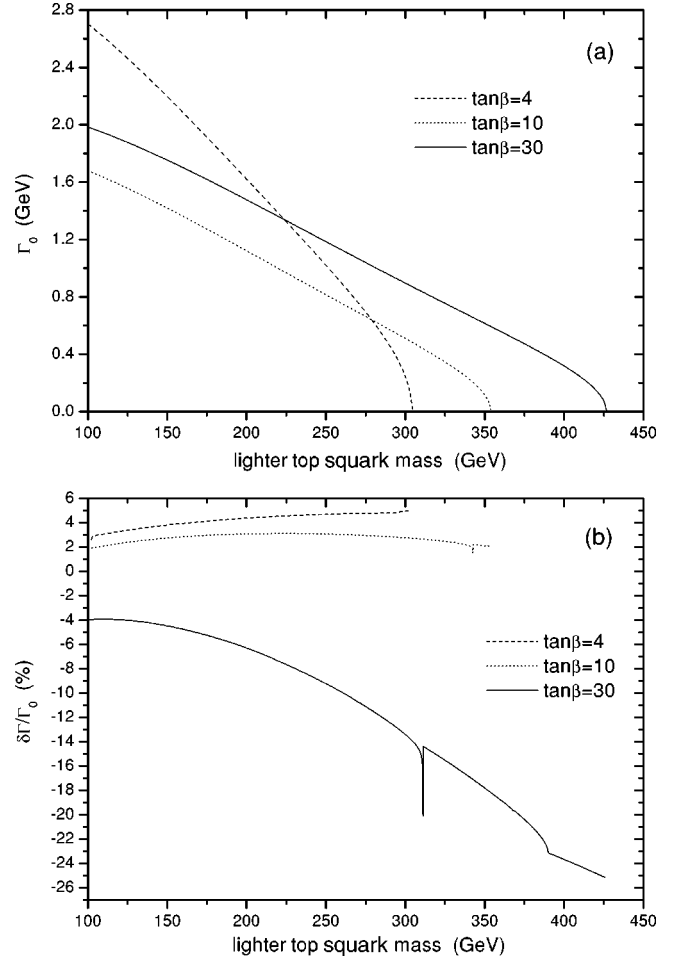


FIG. 4. The tree-level decay width (a) of  $\tilde{b}_2 \rightarrow \tilde{t}_1 H^-$  and its Yukawa corrections (b) as functions of  $m_{\tilde{t}_1}$  for  $\tan\beta = 4, 10$ , and  $30$ , assuming  $m_{A^0} = 150$  GeV,  $\mu = M_2 = 400$  GeV,  $A_t = A_b = 1$  TeV, and  $M_{\tilde{Q}} = M_{\tilde{U}} = M_{\tilde{D}}$ .

perturbation expansion, especially for large  $\tan\beta$ , we take the running mass  $m_b(Q)$  evaluated by the next-to-leading order formula [19]

$$m_b(Q) = U_6(Q, m_t) U_5(m_t, m_b) m_b(m_b), \quad (34)$$

where we have assumed that there are no other colored particles with masses between the scales  $Q$  and  $m_t$ , and  $m_b(m_b) = 4.25$  GeV [20]. The evolution factor  $U_f$  is

$$U_f(Q_2, Q_1) = \left( \frac{\alpha_s(Q_2)}{\alpha_s(Q_1)} \right)^{d^{(f)}} \left[ 1 + \frac{\alpha_s(Q_1) - \alpha_s(Q_2)}{4\pi} J^{(f)} \right], \quad (35)$$

$$d^{(f)} = \frac{12}{33-2f}, \quad J^{(f)} = -\frac{8982 - 504f + 40f^2}{3(33-2f)^2},$$

where  $\alpha_s(Q)$  is given by the solutions of the two-loop renormalization group equations [21]. When  $Q = 400$  GeV, the running mass  $m_b(Q) \sim 2.5$  GeV. In addition, we also improved the perturbation calculations by the following replacement in the tree-level couplings [19]:

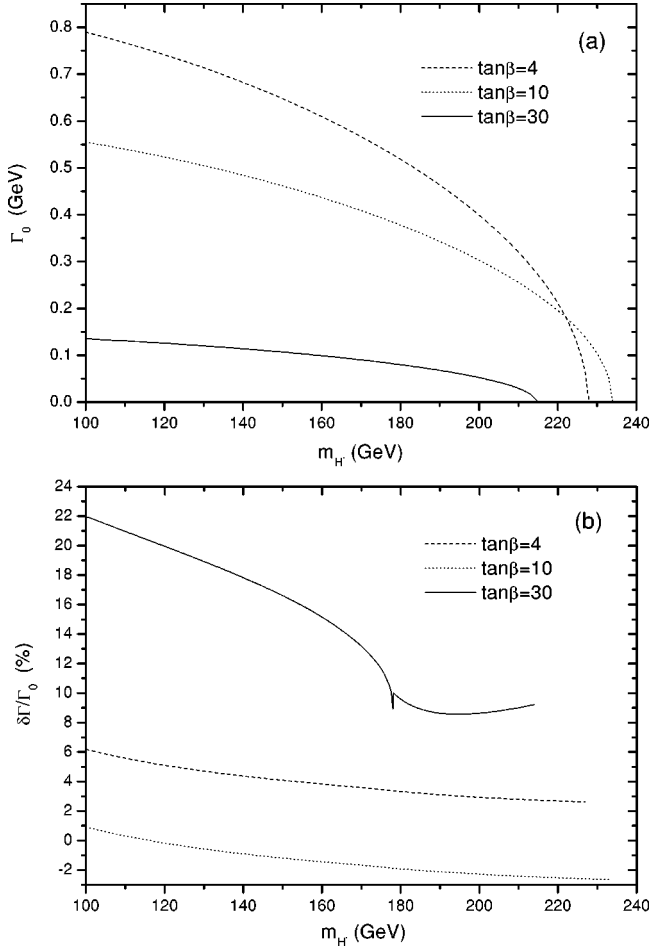


FIG. 5. The tree-level decay width (a) of  $\tilde{b}_1 \rightarrow \tilde{t}_1 H^-$  and its Yukawa corrections (b) as functions of  $m_{H^-}$  for  $\tan\beta = 4, 10,$  and  $30$ , assuming  $m_{\tilde{t}_1} = 170$  GeV,  $\mu = M_2 = 400$  GeV,  $A_t = A_b = 1$  TeV, and  $M_{\tilde{Q}} = M_{\tilde{U}} = M_{\tilde{D}}$ .

$$m_b(Q) \rightarrow \frac{m_b(Q)}{1 + \Delta m_b(M_{\text{SUSY}})}, \quad (36)$$

where

$$\begin{aligned} \Delta m_b = & \frac{2\alpha_s}{3\pi} M_{\tilde{g}} \mu \tan\beta I(m_{\tilde{b}_1}, m_{\tilde{b}_2}, M_{\tilde{g}}) \\ & + \frac{h_t^2}{16\pi^2} \mu A_t \tan\beta I(m_{\tilde{t}_1}, m_{\tilde{t}_2}, \mu) \\ & - \frac{g^2}{16\pi^2} \mu M_2 \tan\beta [\cos^2\theta_{\tilde{t}} I(m_{\tilde{t}_1}, M_2, \mu) \\ & + \sin^2\theta_{\tilde{t}} I(m_{\tilde{t}_2}, M_2, \mu) + \frac{1}{2} \cos^2\theta_{\tilde{b}} I(m_{\tilde{b}_1}, M_2, \mu) \\ & + \frac{1}{2} \sin^2\theta_{\tilde{b}} I(m_{\tilde{b}_2}, M_2, \mu)] \end{aligned} \quad (37)$$

with

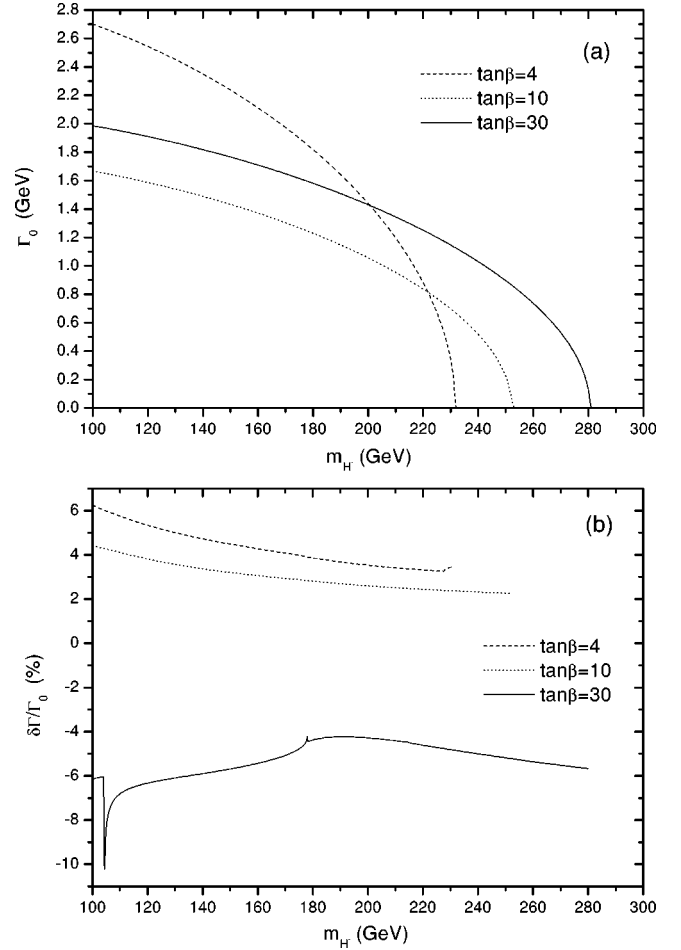


FIG. 6. The tree-level decay width (a) of  $\tilde{b}_2 \rightarrow \tilde{t}_1 H^-$  and its Yukawa corrections (b) as functions of  $m_{H^-}$  for  $\tan\beta = 4, 10,$  and  $30$ , assuming  $m_{\tilde{t}_1} = 170$  GeV,  $\mu = M_2 = 400$  GeV,  $A_t = A_b = 1$  TeV, and  $M_{\tilde{Q}} = M_{\tilde{U}} = M_{\tilde{D}}$ .

$$\begin{aligned} I(a, b, c) = & \frac{1}{(a^2 - b^2)(b^2 - c^2)(a^2 - c^2)} \left( a^2 b^2 \log \frac{a^2}{b^2} \right. \\ & \left. + b^2 c^2 \log \frac{b^2}{c^2} + c^2 a^2 \log \frac{c^2}{a^2} \right). \end{aligned} \quad (38)$$

The two-loop leading-logarithm relations [22] of the neutral Higgs boson masses and mixing angles in the MSSM were used. For  $m_{H^\pm}$  the tree-level formula was used. Other MSSM parameters were determined as follows.

(i) For the parameters  $M_1$ ,  $M_2$ , and  $\mu$  in the chargino and neutralino matrix, we take  $M_2$  and  $\mu$  as the input parameters, and then use the relation  $M_1 = (5/3)(g'^2/g^2)M_2 \approx 0.5M_2$  [2,23] to determine  $M_1$ . The gluino mass  $M_{\tilde{g}}$  in Eq. (37) was related to  $M_2$  by  $M_{\tilde{g}} = (\alpha_s(M_{\tilde{g}})/\alpha_2)M_2$  [5].

(ii) For the parameters  $m_{\tilde{Q}, \tilde{U}, \tilde{D}}$  and  $A_{t,b}$  in squark mass matrices, we assumed  $M_{\tilde{Q}} = M_{\tilde{U}} = M_{\tilde{D}}$  and  $A_t = A_b$  to simplify the calculations.

Some typical numerical results of the tree-level decay

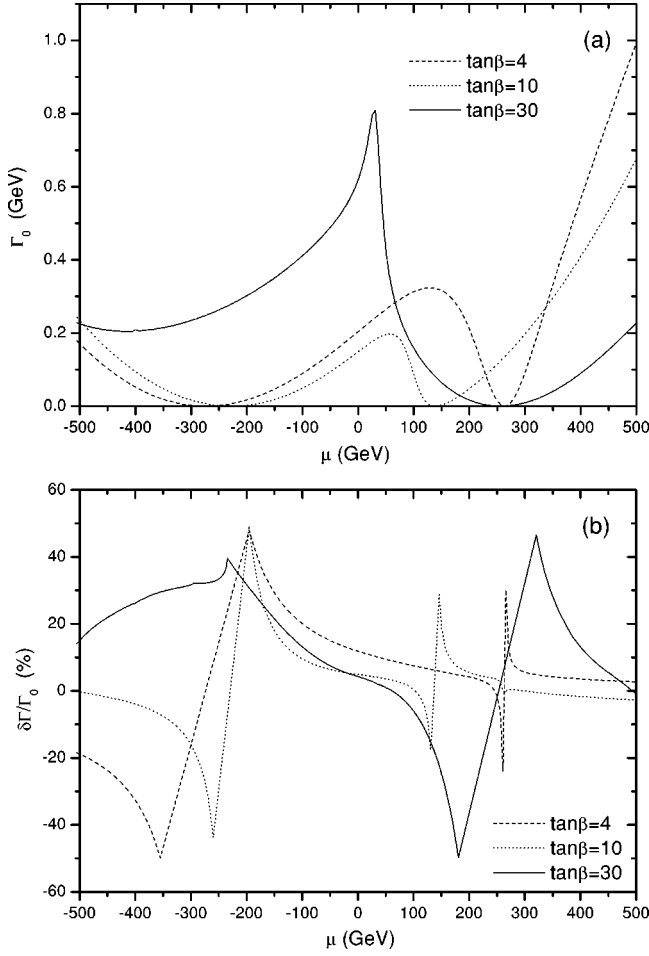


FIG. 7. The tree-level decay width (a) of  $\tilde{b}_1 \rightarrow \tilde{t}_1 H^-$  and its Yukawa corrections (b) as functions of  $\mu$  for  $\tan\beta = 4, 10$ , and  $30$ , assuming  $m_{\tilde{t}_1} = 170$  GeV,  $M_2 = 400$  GeV,  $A_t = A_b = 1$  TeV,  $m_{A^0} = 150$  GeV, and  $M_{\tilde{Q}} = M_{\tilde{U}} = M_{\tilde{D}}$ .

widths and the Yukawa corrections are given in Figs. 3–9 below.

Figures 3 and 4 show the  $m_{\tilde{t}_1}$  dependence of the results of  $\tilde{b}_1$  and  $\tilde{b}_2$  decays, respectively. Here we take  $m_{A^0} = 150$  GeV,  $\mu = M_2 = 400$  GeV, and  $A_t = A_b = 1$  TeV. The leading terms of the tree-level amplitude are given by

$$M_i^{(0)} \sim \frac{ig}{\sqrt{2}m_W} [m_t(A_t \cot\beta + \mu)R_{i1}^{\tilde{b}}R_{i2}^{\tilde{t}} + m_b(A_b \tan\beta + \mu)R_{i2}^{\tilde{b}}R_{i1}^{\tilde{t}}], \quad (39)$$

where  $\cos\theta_{\tilde{b}} \sim (0.54, 0.67, 0.70)$  and  $\cos\theta_{\tilde{t}} \sim (-0.71, -0.71, -0.71)$  for  $\tan\beta = (4, 10, 30)$ , respectively. In the case of  $i = 1$ , the two terms in Eq. (39) have opposite signs, and their magnitudes get close with increasing  $\tan\beta$  and thus cancel to a large extent for large  $\tan\beta$ . Therefore, the tree-level decay widths have the feature  $\Gamma_0(\tan\beta=4) > \Gamma_0(\tan\beta=10) > \Gamma_0(\tan\beta=30)$  in most of the parameter range, as shown in

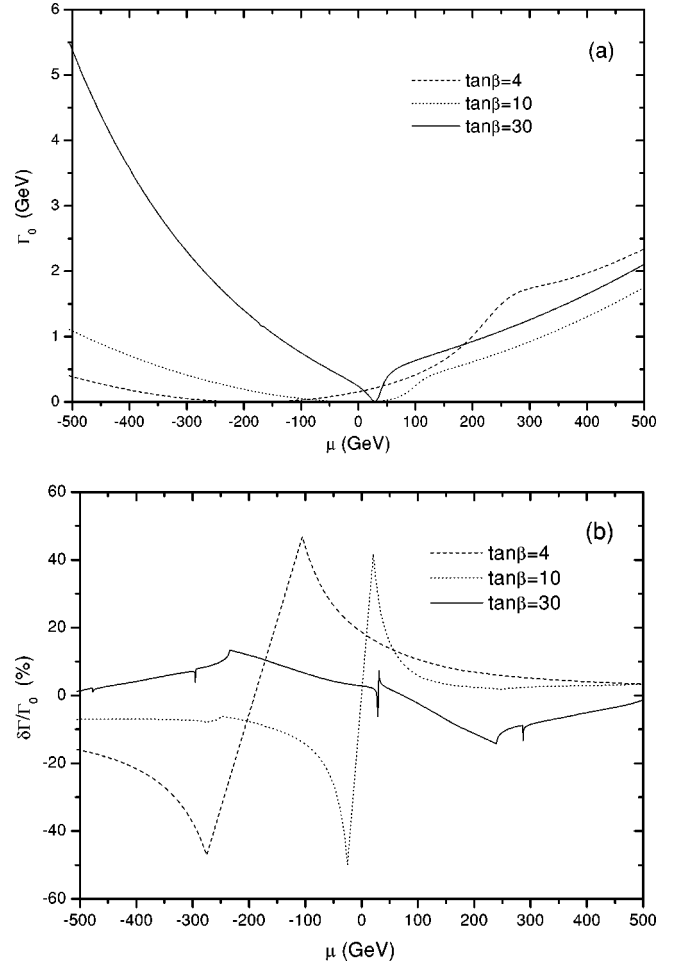


FIG. 8. The tree-level decay width (a) of  $\tilde{b}_2 \rightarrow \tilde{t}_1 H^-$  and its Yukawa corrections (b) as functions of  $\mu$  for  $\tan\beta = 4, 10$ , and  $30$ , assuming  $m_{\tilde{t}_1} = 170$  GeV,  $M_2 = 400$  GeV,  $A_t = A_b = 1$  TeV,  $m_{A^0} = 150$  GeV, and  $M_{\tilde{Q}} = M_{\tilde{U}} = M_{\tilde{D}}$ .

Fig. 3(a). In the case of  $i = 2$ , for  $\tan\beta = 4, 10$ , and  $30$  the two terms in Eq. (39) have the same sign, so  $\Gamma_0$  is larger than for  $i = 1$ . From Figs. 3(b) and 4(b) one can see that the relative corrections are sensitive to the value of  $\tan\beta$ . For  $\tan\beta = 30$ , the magnitudes of the corrections can exceed 10% when  $m_{\tilde{t}_1} > 160$  GeV for  $\tilde{b}_1$  decay and  $m_{\tilde{t}_1} > 260$  GeV for  $\tilde{b}_2$  decay. In particular, in the case of  $\tilde{b}_1$  decay, the correction can even reach 40%, because the corresponding tree-level decay width has already become very small. There are dips at  $m_{\tilde{t}_1} = 311$  and  $390$  GeV on the solid line in Fig. 4(b), which come from the singularities at the threshold points  $m_{\tilde{b}_2} = m_{\tilde{\chi}_1^+} + m_t$  and  $m_{\tilde{b}_1} = m_{\tilde{\chi}_1^+} + m_t$ . However, for  $\tan\beta = 4$  and  $10$ , the corrections to the two bottom squark decays are always small and range from  $-5\%$  to  $5\%$ . In general, for low  $\tan\beta$  the top quark contribution is enhanced while for high  $\tan\beta$  the bottom quark contribution becomes large, and for medium  $\tan\beta$  there are no enhanced effects from Yukawa couplings. So the corrections for  $\tan\beta = 4$  are generally larger than those for  $\tan\beta = 10$ , as shown in Figs. 3(b) and 4(b).

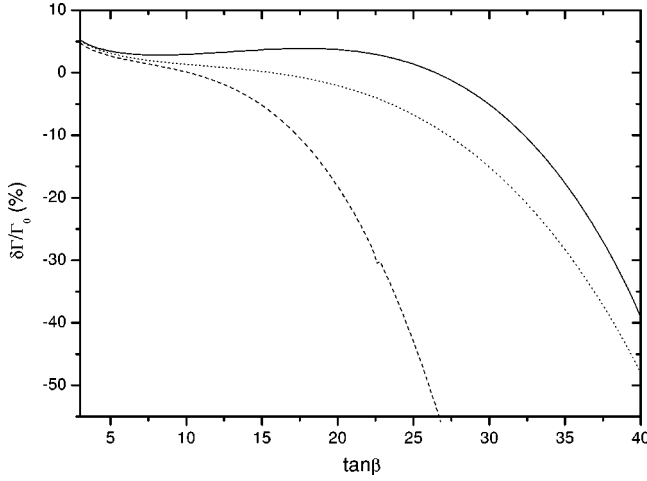


FIG. 9. The Yukawa corrections of  $\tilde{b}_2 \rightarrow \tilde{t}_1 H^-$  as a function of  $\tan\beta$ , assuming  $m_{\tilde{t}_1} = 170$  GeV,  $\mu = M_2 = 400$  GeV,  $A_t = A_b = 1$  TeV,  $m_{A^0} = 150$  GeV, and  $M_{\tilde{Q}} = M_{\tilde{U}} = M_{\tilde{D}}$ . The dashed line corresponds to the corrections using the on-shell bottom quark mass, the dotted line to the improved result using only the QCD running mass  $m_b(Q)$ , and the solid line to the improved result using the replacement Eq. (36).

Figure 5 (Fig. 6) gives the tree-level decay width and the Yukawa corrections as functions of  $m_{H^-}$  in the case of  $\tilde{b}_1$  decay ( $\tilde{b}_2$  decay). We assumed  $m_{\tilde{t}_1} = 170$  GeV,  $\mu = M_2 = 400$  GeV, and  $A_t = A_b = 1$  TeV. The features of the tree-level decay widths in Figs. 5(a) and 6(a) are similar to those of Figs. 3(a) and 4(a), respectively. From Figs. 5(b) and 6(b) we can see that the corrections decrease or increase the decay widths depending on  $\tan\beta$ . Figure 5(b) shows that the corrections for  $\tan\beta=4$  are always positive and range between 6% and 3%. For  $\tan\beta=10$  the corrections are negligibly small. For high  $\tan\beta$  ( $=30$ ) the corrections exceed 10% when  $m_{H^-} < 180$  GeV. There is a dip at  $m_{H^-} \sim 178$  GeV on the solid curve due to the singularity of the charged Higgs boson wave function renormalization constant at the threshold point  $m_{H^-} = m_t + m_b$ . Figure 6(b) shows that the corrections are a few percent for  $\tan\beta=4, 10$ , and  $30$ . There are a dip and a peak on the solid curve, which arise from the singularities at the threshold points  $m_{\tilde{b}_2} = m_{\tilde{b}_1} + m_{A^0}$  and  $m_{H^-} = m_t + m_b$ , respectively.

In Figs. 7 and 8 we present the tree-level decay widths and the Yukawa corrections as functions of  $\mu$  in the cases of  $\tilde{b}_1 \rightarrow \tilde{t}_1 + H^-$  and  $\tilde{b}_2 \rightarrow \tilde{t}_1 + H^-$ , respectively, assuming  $m_{\tilde{t}_1} = 170$  GeV,  $M_2 = 400$  GeV,  $A_t = A_b = 1$  TeV, and  $m_{A^0} = 150$  GeV. When  $\mu$  takes certain values, the tree-level decay widths become very small ( $< 10^{-3}$  GeV), as shown in Figs. 7(a) and 8(a), and the corrections near these values do not have a physical meaning. So we cut off the corrections, since perturbation theory breaks down there. From Fig. 7(a) [Fig. 8(a)] we can see that there is a high peak (a deep dip) for  $\tan\beta=30$  and  $\mu \sim 30$  GeV. This is because when  $\tan\beta=30$  and  $\mu \sim 30$  GeV the second term in Eq. (39) is enhanced (suppressed) greatly for  $\sin\theta_b \sim 1$  ( $\cos\theta_b \sim 0$ ) as a result of

the off-diagonal elements of  $M_b^2$  in Eq. (2) approaching zero. Figures 7(b) and 8(b) show that the Yukawa corrections depend strongly on  $\mu$ . In particular, when  $\Gamma_0$  becomes very small, the corrections have rapid variations between positive and negative values with changes in the sign of the tree-level amplitude. In general, when the tree-level decay widths for  $\tan\beta=4$  and  $10$  are not close to zero, the corrections are always small. Comparing Fig. 7(b) with Fig. 8(b), we find that the Yukawa corrections for  $\tan\beta=30$  are more significant for  $\tilde{b}_1$  decay than for  $\tilde{b}_2$  decay.

Finally, in Fig. 9 we show the Yukawa corrections as a function of  $\tan\beta$  from three methods of perturbative expansion: (i) the strict on-shell scheme (the dashed line), where the bottom quark pole mass  $4.7$  GeV was used, (ii) the QCD-improved scheme (the dotted line), in which only the QCD running bottom quark mass  $m_b(Q)$  in Eq. (34) was used, and (iii) the improved scheme (the solid line), in which the replacement Eq. (36) was used. Here we assumed  $m_{\tilde{t}_1} = 170$  GeV,  $\mu = M_2 = 400$  GeV,  $A_t = A_b = 1$  TeV, and  $m_{A^0} = 150$  GeV. One can see that the three methods all give small corrections ( $|\delta\Gamma/\Gamma_0| < 5\%$ ) for  $\tan\beta < 15$ . However, the magnitude of the corrections in case (i) increases rapidly for  $\tan\beta > 15$ , and when  $\tan\beta > 33$  the corrections result in a physically meaningless negative width. But the convergences in the cases (ii) and (iii) are much better, and especially in the case (iii) the magnitude of the corrections is still less than 40% for high values of  $\tan\beta$  ( $=40$ ).

In conclusion, we have calculated the Yukawa corrections to the width of the bottom squark decay into a lighter top squark plus a charged Higgs boson in the MSSM. These corrections depend on the masses of the charged Higgs boson and the lighter top squark and the parameters  $\tan\beta$  and  $\mu$ . For favorable parameter values, the corrections decrease or increase the decay widths significantly. In particular, for high values of  $\tan\beta$  ( $=30$ ) the corrections exceed 10% for both  $\tilde{b}_1$  and  $\tilde{b}_2$  decay. But for low values of  $\tan\beta$  ( $=4, 10$ ) the corrections are small and the magnitudes are less than 10%. The numerical calculations also show that using the running bottom quark mass, which includes the QCD effects and resumes all high order ( $\tan\beta$ )-enhanced effects, as given in Ref. [19], can greatly improve the convergence of the perturbation expansion.

## ACKNOWLEDGMENTS

We thank Ya Sheng Yang for giving help in the numerical calculations. This work was supported in part by the National Natural Science Foundation of China, the Doctoral Program Foundation of Higher Education of China, and a grant from the State Commission of Science and Technology of China.

## APPENDIX A

The following couplings are given to order  $\mathcal{O}(h_t, h_b)$ .



**1. Squark–squark–Higgs boson**

 (a) Squark-squark- $h^0$ :

$$\hat{G}_1^{\tilde{q}} = \begin{pmatrix} -\sqrt{2}m_q h_q \begin{Bmatrix} c_\alpha \\ -s_\alpha \end{Bmatrix} & -\frac{1}{\sqrt{2}}h_q \left( A_q \begin{Bmatrix} c_\alpha \\ -s_\alpha \end{Bmatrix} + \mu \begin{Bmatrix} s_\alpha \\ c_\alpha \end{Bmatrix} \right) \\ -\frac{1}{\sqrt{2}}h_q \left( A_q \begin{Bmatrix} c_\alpha \\ -s_\alpha \end{Bmatrix} + \mu \begin{Bmatrix} s_\alpha \\ c_\alpha \end{Bmatrix} \right) & -\sqrt{2}m_q h_q \begin{Bmatrix} c_\alpha \\ -s_\alpha \end{Bmatrix} \end{pmatrix} \quad (\text{A1})$$

 for  $\begin{Bmatrix} \text{up} \\ \text{down} \end{Bmatrix}$  type squarks, respectively. We use the abbreviations  $s_\alpha = \sin \alpha$ ,  $c_\alpha = \cos \alpha$ .  $\alpha$  is the mixing angle in the  $CP$ -even neutral Higgs boson sector.

 (b) Squark-squark- $H^0$ :

$$\hat{G}_2^{\tilde{q}} = \begin{pmatrix} -\sqrt{2}m_q h_q \begin{Bmatrix} s_\alpha \\ c_\alpha \end{Bmatrix} & -\frac{1}{\sqrt{2}}h_q \left( A_q \begin{Bmatrix} s_\alpha \\ c_\alpha \end{Bmatrix} - \mu \begin{Bmatrix} c_\alpha \\ s_\alpha \end{Bmatrix} \right) \\ -\frac{1}{\sqrt{2}}h_q \left( A_q \begin{Bmatrix} s_\alpha \\ c_\alpha \end{Bmatrix} - \mu \begin{Bmatrix} c_\alpha \\ s_\alpha \end{Bmatrix} \right) & -\sqrt{2}m_q h_q \begin{Bmatrix} s_\alpha \\ c_\alpha \end{Bmatrix} \end{pmatrix}. \quad (\text{A2})$$

 (c) Squark-squark- $A^0$ :

$$\hat{G}_3^{\tilde{q}} = i \frac{gm_q}{2m_W} \begin{pmatrix} 0 & -A_q \begin{Bmatrix} \cot \beta \\ \tan \beta \end{Bmatrix} - \mu \\ A_q \begin{Bmatrix} \cot \beta \\ \tan \beta \end{Bmatrix} + \mu & 0 \end{pmatrix}. \quad (\text{A3})$$

 (d) Squark-squark- $G^0$ :

$$\hat{G}_4^{\tilde{q}} = i \frac{gm_q}{2m_W} \begin{pmatrix} 0 & -A_q + \mu \begin{Bmatrix} \cot \beta \\ \tan \beta \end{Bmatrix} \\ A_q - \mu \begin{Bmatrix} \cot \beta \\ \tan \beta \end{Bmatrix} & 0 \end{pmatrix}. \quad (\text{A4})$$

 (e) Squark-squark- $H^\pm$ :

$$\hat{G}_5^{\tilde{b}} = (\hat{G}_5^{\tilde{t}})^T = \frac{g}{\sqrt{2}m_W} \begin{pmatrix} m_b^2 \tan \beta + m_t^2 \cot \beta & m_t(A_t \cot \beta + \mu) \\ m_b(A_b \tan \beta + \mu) & 2m_t m_b / \sin 2\beta \end{pmatrix}. \quad (\text{A5})$$

 (f) Squark-squark- $G^\pm$ :

$$\hat{G}_6^{\tilde{b}} = (\hat{G}_6^{\tilde{t}})^T = \frac{g}{\sqrt{2}m_W} \begin{pmatrix} m_t^2 - m_b^2 & m_t(A_t - \mu \cot \beta) \\ m_b(\mu \tan \beta - A_b) & 0 \end{pmatrix}. \quad (\text{A6})$$

**2. Quark–quark–Higgs boson**

$$a_k^q = \left( \frac{1}{\sqrt{2}}h_q \begin{Bmatrix} -c_\alpha \\ s_\alpha \end{Bmatrix}, -\frac{1}{\sqrt{2}}h_q \begin{Bmatrix} s_\alpha \\ c_\alpha \end{Bmatrix}, -\frac{i}{\sqrt{2}}h_q \begin{Bmatrix} \cos \beta \\ \sin \beta \end{Bmatrix}, \frac{ig}{2m_W} \begin{Bmatrix} -m_t \\ m_b \end{Bmatrix}, \begin{Bmatrix} h_b \sin \beta \\ h_t \cos \beta \end{Bmatrix}, \frac{g}{\sqrt{2}m_W} \begin{Bmatrix} -m_b \\ m_t \end{Bmatrix} \right), \quad (\text{A7})$$

$$b_k^q = \left( \frac{1}{\sqrt{2}}h_q \begin{Bmatrix} -c_\alpha \\ s_\alpha \end{Bmatrix}, -\frac{1}{\sqrt{2}}h_q \begin{Bmatrix} s_\alpha \\ c_\alpha \end{Bmatrix}, -\frac{i}{\sqrt{2}}h_q \begin{Bmatrix} \cos \beta \\ \sin \beta \end{Bmatrix}, \frac{ig}{2m_W} \begin{Bmatrix} m_t \\ -m_b \end{Bmatrix}, h_q \begin{Bmatrix} \cos \beta \\ h_t \sin \beta \end{Bmatrix}, \frac{g}{\sqrt{2}m_W} \begin{Bmatrix} m_t \\ -m_b \end{Bmatrix} \right). \quad (\text{A8})$$

### 3. Quark-squark-neutralino

$$a_{ik}^{\tilde{q}} = -R_{i2}^{\tilde{q}} Y_q \begin{Bmatrix} N_{k4} \\ N_{k3} \end{Bmatrix}, \quad b_{ik}^{\tilde{q}} = -R_{i1}^{\tilde{q}} Y_q \begin{Bmatrix} N_{k4}^* \\ N_{k3}^* \end{Bmatrix}. \quad (\text{A9})$$

Here  $N$  is the  $4 \times 4$  unitary matrix diagonalizing the neutral gaugino-Higgsino mass matrix [2,23], and the Yukawa factor  $Y_q = h_q/g$ .

### 4. Quark-squark-chargino

$$l_{ik}^{\tilde{q}} = R_{i2}^{\tilde{q}} Y_q \begin{Bmatrix} V_{k2} \\ U_{k2} \end{Bmatrix}, \quad k_{ik}^{\tilde{q}} = R_{i1}^{\tilde{q}} \begin{Bmatrix} Y_b U_{k2} \\ Y_t V_{k2} \end{Bmatrix}. \quad (\text{A10})$$

Here  $U$  and  $V$  are the  $2 \times 2$  unitary matrices diagonalizing the charged gaugino-Higgsino mass matrix [2,23].

### 5. Squark-squark-Higgs boson-Higgs boson

(a) Squark-squark- $H^- - H_k$  ( $k = 1, \dots, 4$ ):

$$\hat{G}_{5k}^{\tilde{b}} = (\hat{G}_{5k}^{\tilde{t}})^T = \frac{g^2}{2\sqrt{2}m_W^2} \begin{pmatrix} m_t^2 S_k + m_b^2 T_k & 0 \\ 0 & 2m_t m_b / \sin 2\beta V_k \end{pmatrix} \quad (\text{A11})$$

with

$$S_k = (\cos \alpha \cos \beta / \sin^2 \beta, \sin \alpha \cos \beta / \sin^2 \beta, \\ -i \cot^2 \beta, i \cot \beta), \quad (\text{A12})$$

$$T_k = (-\sin \alpha \sin \beta / \cos^2 \beta, \cos \alpha \sin \beta / \cos^2 \beta, \\ \times i \tan^2 \beta, i \tan \beta), \quad (\text{A13})$$

$$V_k = (\sin(\beta - \alpha), \cos(\beta - \alpha), 0, i). \quad (\text{A14})$$

(b) Squark-squark- $H^- - H^+$ :

$$\hat{G}_{55}^{\tilde{q}} = \begin{pmatrix} -\begin{Bmatrix} h_b^2 \sin^2 \beta \\ h_t^2 \cos^2 \beta \end{Bmatrix} & 0 \\ 0 & -h_q^2 \begin{Bmatrix} \cos^2 \beta \\ \sin^2 \beta \end{Bmatrix} \end{pmatrix}. \quad (\text{A15})$$

(c) Squark-squark- $H^- - G^+$ :

$$\hat{G}_{56}^{\tilde{q}} = -\frac{g^2}{2m_W^2} \begin{pmatrix} \begin{Bmatrix} -m_b^2 \tan \beta \\ m_t^2 \cot \beta \end{Bmatrix} & 0 \\ 0 & m_q^2 \begin{Bmatrix} \cot \beta \\ -\tan \beta \end{Bmatrix} \end{pmatrix}. \quad (\text{A16})$$

## APPENDIX B

We define  $q = t$  and  $b$ ,  $q'$  the  $SU(2)_L$  partner of  $q$ , and  $q'' = q$  for  $k = 1, \dots, 4$  and  $q'' = q'$  for  $k = 5, 6$ . Then we have

$$\frac{\delta m_W^2}{m_W^2} = \frac{g^2}{16\pi^2 m_W^2} [m_b^2 + m_t^2 - A_0(m_t^2) - A_0(m_b^2) - m_t^2 B_0 - (m_t^2 - m_b^2) B_1] (m_W^2, m_b, m_t),$$

$$\frac{\delta m_Z^2}{m_Z^2} = \frac{3g^2}{8\pi^2 m_W^2} \sum_{q=t,b} \left\{ \frac{1}{3} [(I_{3L}^q - e_q \sin^2 \theta_W)^2 + e_q^2 \sin^4 \theta_W] [2m_q^2 - 2A_0(m_q^2) - m_q^2 B_0] - 2m_q^2 e_q \sin^2 \theta_W \right. \\ \left. \times (I_{3L}^q - e_q \sin^2 \theta_W) B_0 \right\} (m_Z^2, m_q, m_q),$$

$$\delta Z_{H^-} = \frac{3}{16\pi^2} \left\{ 2[(a_5^t b_5^b + b_5^t a_5^b)(m_{H^+}^2 + G_1 + B_1 + m_b^2 G_0) + m_t m_b (a_5^t a_5^b + b_5^t b_5^b) G_0] (m_{H^+}^2, m_b, m_t) \right. \\ \left. - \sum_{j,l} (G_5^{\tilde{b}})_{jl} (G_5^{\tilde{t}})_{lj} G_0 (m_{H^+}^2, m_{\tilde{b}_l}, m_{\tilde{t}_j}) \right\},$$

$$T_{H_k} = \frac{3}{16\pi^2} \sum_{q=t,b} \left\{ 2(a_k^q + b_k^q) m_q A_0(m_q^2) - \sum_j (G_k^{\tilde{q}})_{jj} A_0(m_{q_j}^2) \right\},$$

$$\Sigma_{GH} = -\frac{3}{16\pi^2} \left( 2\{(a_5^t b_6^b + b_5^t a_6^b)[m_{H^+}^2 + B_1 + A_0(m_t^2) + m_b^2 B_0] + m_t m_b (a_5^t a_6^b + b_5^t b_6^b) B_0\} (m_{H^+}^2, m_b, m_t) \right. \\ \left. - \sum_{j,l} (G_5^{\tilde{t}})_{jl} (G_6^{\tilde{b}})_{lj} B_0 (m_{H^+}^2, m_{\tilde{b}_l}, m_{\tilde{t}_j}) + \sum_{q=t,b} \sum_j (G_{56}^{\tilde{q}})_{jj} A_0(m_{q_j}^2) \right),$$

$$\frac{\delta m_q}{m_q} = \frac{1}{16\pi^2} \left\{ \sum_{k=1}^6 \left[ \frac{m_{q''}}{m_q} a_k^q a_k^{q''} B_0 - \frac{1}{2} (a_k^q b_k^{q''} + b_k^q a_k^{q''}) B_1 \right] (m_q^2, m_{q''}, m_{H_k}) + g^2 \sum_{k=1}^4 \sum_j \left[ \frac{m_{\tilde{\chi}_k^0}}{m_q} a_{jk}^{\tilde{q}} b_{jk}^{\tilde{q}*} B_0 - \frac{1}{2} (|a_{jk}^{\tilde{q}}|^2 + |b_{jk}^{\tilde{q}}|^2) B_1 \right] (m_q^2, m_{\tilde{\chi}_k^0}, m_{\tilde{q}_j}) + g^2 \sum_{k=1}^2 \sum_j \left[ \frac{m_{\tilde{\chi}_k^+}}{m_q} l_{jk}^{\tilde{q}'} k_{jk}^{\tilde{q}'*} B_0 - \frac{1}{2} (|l_{jk}^{\tilde{q}'}|^2 + |k_{jk}^{\tilde{q}'*}|^2) B_1 \right] (m_q^2, m_{\tilde{\chi}_k^+}, m_{\tilde{q}_j}) \right\},$$

$$\delta m_{\tilde{q}_i}^2 = \frac{1}{16\pi^2} \left( \sum_{k=1}^6 \sum_j (G_k^{\tilde{q}})_{ij} (G_k^{\tilde{q}''})_{ji} B_0 (m_{\tilde{q}_i}^2, m_{\tilde{q}_j}, m_{H_k}) - 2g^2 \sum_{k=1}^4 \{ (|a_{ik}^{\tilde{q}}|^2 + |b_{ik}^{\tilde{q}}|^2) [m_{\tilde{q}_i}^2 B_1 + A_0 (m_{\tilde{\chi}_k^0}^2) + m_q^2 B_0] + 2m_q m_{\tilde{\chi}_k^0} \operatorname{Re}(a_{ik}^{\tilde{q}} b_{ik}^{\tilde{q}*}) B_0 \} (m_{\tilde{q}_i}^2, m_q, m_{\tilde{\chi}_k^0}) - 2g^2 \sum_{k=1}^2 \{ (|l_{ik}^{\tilde{q}'}|^2 + |k_{ik}^{\tilde{q}'*}|^2) [m_{\tilde{q}_i}^2 B_1 + A_0 (m_{\tilde{\chi}_k^+}^2) + m_q^2 B_0] + 2m_q m_{\tilde{\chi}_k^+} \operatorname{Re}(l_{ik}^{\tilde{q}'} k_{ik}^{\tilde{q}'*}) B_0 \} (m_{\tilde{q}_i}^2, m_{q'}, m_{\tilde{\chi}_k^+}) \right),$$

$$\delta Z_{\tilde{q}_i} = \frac{1}{16\pi^2} \left\{ - \sum_{k=1}^6 \sum_j (G_k^{\tilde{q}})_{ij} (G_k^{\tilde{q}''})_{ji} G_0 (m_{\tilde{q}_i}^2, m_{\tilde{q}_j}, m_{H_k}) + 2g^2 \sum_{k=1}^4 [ (|a_{ik}^{\tilde{q}}|^2 + |b_{ik}^{\tilde{q}}|^2) (B_1 + m_{\tilde{q}_i}^2 G_1 + m_q^2 G_0) + 2m_q m_{\tilde{\chi}_k^0} \operatorname{Re}(a_{ik}^{\tilde{q}} b_{ik}^{\tilde{q}*}) G_0 ] (m_{\tilde{q}_i}^2, m_q, m_{\tilde{\chi}_k^0}) + 2g^2 \sum_{k=1}^2 [ (|l_{ik}^{\tilde{q}'}|^2 + |k_{ik}^{\tilde{q}'*}|^2) (B_1 + m_{\tilde{q}_i}^2 G_1 + m_q^2 G_0) + 2m_q m_{\tilde{\chi}_k^+} \operatorname{Re}(l_{ik}^{\tilde{q}'} k_{ik}^{\tilde{q}'*}) G_0 ] (m_{\tilde{q}_i}^2, m_{q'}, m_{\tilde{\chi}_k^+}) \right\},$$

$$\Sigma_{12}^{\tilde{q}}(p^2) = \frac{1}{16\pi^2} \left( \sum_{k=1}^6 \sum_j (G_k^{\tilde{q}})_{1j} (G_k^{\tilde{q}''})_{j2} B_0 (p^2, m_{\tilde{q}_j}, m_{H_k}) - 2g^2 \sum_{k=1}^4 \{ (a_{1k}^{\tilde{q}} a_{2k}^{\tilde{q}*} + b_{1k}^{\tilde{q}} b_{2k}^{\tilde{q}*}) [p^2 B_1 + A_0 (m_{\tilde{\chi}_k^0}^2) + m_q^2 B_0] + m_q m_{\tilde{\chi}_k^0} (a_{1k}^{\tilde{q}} b_{2k}^{\tilde{q}*} + a_{2k}^{\tilde{q}*} b_{1k}^{\tilde{q}}) B_0 \} (p^2, m_q, m_{\tilde{\chi}_k^0}) - 2g^2 \sum_{k=1}^2 [ (l_{1k}^{\tilde{q}'} l_{2k}^{\tilde{q}'*} + k_{1k}^{\tilde{q}'*} k_{2k}^{\tilde{q}'}) \times (p^2 B_1 + A_0 (m_{\tilde{\chi}_k^+}^2) + m_q^2 B_0) + m_q m_{\tilde{\chi}_k^+} (l_{1k}^{\tilde{q}'} k_{2k}^{\tilde{q}'*} + l_{2k}^{\tilde{q}'*} k_{1k}^{\tilde{q}'}) B_0 ] (p^2, m_{q'}, m_{\tilde{\chi}_k^+}) \right),$$

$$\delta\theta_{\tilde{q}} + \delta Z_{21}^{\tilde{q}} = \frac{1}{2(m_{\tilde{q}_1}^2 - m_{\tilde{q}_2}^2)} [\Sigma_{12}^{\tilde{q}}(m_{\tilde{q}_2}^2) - \Sigma_{12}^{\tilde{q}}(m_{\tilde{q}_1}^2)],$$

$$\Pi_{ij}^L(p^2) = - \frac{3}{16\pi^2} \sum_{k=1}^2 [ l_{ki}^{\tilde{t}} l_{kj}^{\tilde{t}} B_1(p^2, m_b, m_{\tilde{t}_k}) + k_{ki}^{\tilde{b}} k_{kj}^{\tilde{b}} B_1(p^2, m_t, m_{\tilde{b}_k}) ],$$

$$\Pi_{ij}^R(p^2) = - \frac{3}{16\pi^2} \sum_{k=1}^2 [ k_{ki}^{\tilde{t}} k_{kj}^{\tilde{t}} B_1(p^2, m_b, m_{\tilde{t}_k}) + l_{ki}^{\tilde{b}} l_{kj}^{\tilde{b}} B_1(p^2, m_t, m_{\tilde{b}_k}) ],$$

$$\Pi_{ij}^{S,L}(p^2) = \frac{3}{16\pi^2} \sum_{k=1}^2 [ m_b k_{ki}^{\tilde{t}} l_{kj}^{\tilde{t}} B_0(p^2, m_b, m_{\tilde{t}_k}) + m_t l_{ki}^{\tilde{b}} k_{kj}^{\tilde{b}} B_0(p^2, m_t, m_{\tilde{b}_k}) ],$$

$$\Pi_{ij}^{S,R}(p^2) = \frac{3}{16\pi^2} \sum_{k=1}^2 [ m_b l_{ki}^{\tilde{t}} k_{kj}^{\tilde{t}} B_0(p^2, m_b, m_{\tilde{t}_k}) + m_t k_{ki}^{\tilde{b}} l_{kj}^{\tilde{b}} B_0(p^2, m_t, m_{\tilde{b}_k}) ].$$

Here  $A_0$  and  $B_1$  are one- and two-point Feynman integrals [14], respectively, and  $G_i = \partial B_i / \partial p^2$ .

- [1] H. P. Nilles, *Phys. Rep.* **110**, 1 (1984); A. B. Lahanas and D. V. Nanopoulos, *ibid.* **145**, 1 (1987); *Supersymmetry*, Vols. 1 and 2, edited by S. Ferrara (North Holland/World Scientific, Singapore, 1987).
- [2] H. E. Haber and G. L. Kane, *Phys. Rep.* **117**, 75 (1985).
- [3] H. Baer, V. Barger, D. Karatas, and X. Tata, *Phys. Rev. D* **36**, 96 (1987); K. Hikasa and M. Kobayashi, *ibid.* **36**, 724 (1987); R. M. Barnett, J. F. Gunion, and H. E. Haber, *ibid.* **37**, 1892 (1988); H. Baer, X. Tata, and J. Woodside, *ibid.* **42**, 1568 (1990); K. Hikasa and M. Drees, *Phys. Lett. B* **252**, 127 (1990); A. Bartl, W. Majerotto, B. Mösslacher, and N. Oshimo, *Z. Phys. C* **52**, 477 (1991); A. Bartl, W. Majerotto, and W. Porod, *ibid.* **64**, 499 (1994); **68**, 518(E) (1995).
- [4] A. Bartl, H. Eberl, K. Hidaka, S. Kraml, T. Kon, W. Majerotto, W. Porod, and Y. Yamada, *Phys. Lett. B* **435**, 118 (1998).
- [5] K. Hidaka and A. Bartl, *Phys. Lett. B* **501**, 78 (2001).
- [6] Atlas Collaboration, Atlas Technical Design Report No. CERN/LHCC/99-14/15; CMS Collaboration, CMS Technical Proposal No. CERN/LHCC/94-38; F. Gianotti, in *Proceedings of the IVth International Symposium on Radiative Corrections (RADCOR 98)*, edited by J. Solà (World Scientific, Singapore, 1999), p. 270.
- [7] D. J. Miller, in *Proceedings of the IVth International Symposium on Radiative Corrections (RADCOR 98)* (Ref. [6]), p. 289.
- [8] S. Kraml, H. Eberl, A. Bartl, W. Majerotto, and W. Porod, *Phys. Lett. B* **386**, 175 (1996); A. Djouadi, W. Hollik, and C. Jünger, *Phys. Rev. D* **55**, 6975 (1997); A. Bartl, H. Eberl, K. Hidaka, S. Kraml, W. Majerotto, W. Porod, and Y. Yamada, *ibid.* **59**, 115007 (1999).
- [9] J. Guasch, W. Hollik, and J. Solà, *Phys. Lett. B* **437**, 88 (1998).
- [10] J. Guasch, W. Hollik, and J. Solà, *Phys. Lett. B* **510**, 211 (2001).
- [11] S. Sirlin, *Phys. Rev. D* **22**, 971 (1980); W. J. Marciano and A. Sirlin, *ibid.* **22**, 2695 (1980); **31**, 213(E) (1985); A. Sirlin and W. J. Marciano, *Nucl. Phys.* **B189**, 442 (1981); K. I. Aoki *et al.*, *Prog. Theor. Phys. Suppl.* **73**, 1 (1982).
- [12] R. Santos and A. Barroso, *Phys. Rev. D* **56**, 5366 (1997).
- [13] A. Mendez and A. Pomarol, *Phys. Lett. B* **279**, 98 (1992).
- [14] G. 't Hooft and M. Veltman, *Nucl. Phys.* **B44**, 189 (1972); G. Passarino and M. Veltman, *ibid.* **B160**, 151 (1979); A. Axelrod, *ibid.* **B209**, 349 (1982); M. Clements *et al.*, *Phys. Rev. D* **27**, 570 (1983).
- [15] A. Bartl, H. Eberl, K. Hidaka, T. Kon, W. Majerotto, and Y. Yamada, *Phys. Lett. B* **402**, 303 (1997).
- [16] D. Pierce and A. Papadopoulos, *Phys. Rev. D* **50**, 565 (1994).
- [17] H. Eberl, M. Kincel, W. Majerotto, and Y. Yamada, *Phys. Rev. D* **64**, 115013 (2001).
- [18] Particle Data Group, *C. Caso et al.*, *Eur. Phys. J. C* **3**, 1 (1998).
- [19] M. Carena, D. Garcia, U. Nierste, and C. E. M. Wagner, *Nucl. Phys.* **B577**, 88 (2000).
- [20] M. Beneke and A. Signer, *Phys. Lett. B* **471**, 233 (1999); A. H. Hoang, *Phys. Rev. D* **61**, 034005 (2000).
- [21] S. G. Gorishny, A. L. Kataev, S. A. Larin, and L. R. Surguladze, *Mod. Phys. Lett. A* **5**, 2703 (1990); *Phys. Rev. D* **43**, 1633 (1991); A. Djouadi, M. Spira, and P. M. Zerwas, *Z. Phys. C* **70**, 427 (1996); A. Djouadi, J. Kalinowski, and M. Spira, *Comput. Phys. Commun.* **108**, 56 (1998); M. Spira, *Fortschr. Phys.* **46**, 203 (1998).
- [22] M. Carena, M. Quirós, and C. E. M. Wagner, *Nucl. Phys.* **B461**, 407 (1996).
- [23] P. Nath, R. Arnowitt, and A. Chamseddine, *Applied N=1 Supergravity*, ICTP Series in Theoretical Physics (World Scientific, Singapore, 1984); J. F. Gunion and H. E. Haber, *Nucl. Phys.* **B272**, 1 (1986); L. E. Ibáñez and G. G. Ross, in *Perspectives on Higgs Physics*, edited by G. L. Kane (World Scientific, Singapore, 1993), hep-ph/9204201.